High-spin states in ^{76}Br

D. F. Winchell, L. Wehner, J. X. Saladin, M. S. Kaplan,* and E. Landulfo†
Department of Physics and Astronomy, University of Pittsburgh, Pittsburgh, Pennsylvania 15260

A. Aprahamian
Physics Department, University of Notre Dame, Notre Dame, Indiana 46556

(Received 22 July 1996)

High-spin states in the odd-odd nucleus ^{76}Br were populated with two different reactions: ^{63}Cu(^{16}O,$n2p$) and ^{63}Cu(^{19}F,αpn). The Pitt multidetector array was used to collect γ-γ coincidence data. The level scheme has been extended considerably. The features of the level scheme, particularly the signature inversions in the yrast band, are compared to the results of cranked Woods-Saxon shell-model calculations with self-consistent pairing. [S0556-2813(97)00801-7]

PACS number(s): 21.10.Re, 21.60.Cs, 23.20.Lv, 27.50.+e

I. INTRODUCTION

The study of high angular momentum states in deformed nuclei in the mass $A \approx 80$ region has been a topic of considerable interest. The deformation of nuclei in this mass region and therefore the structure of high-spin states are found to depend strongly on Z and N. In particular, it is found that an unpaired nucleon can polarize the shape of the nucleus, causing differences between nuclei with even Z and N and those with unpaired nucleons. Early investigations of the even-even nuclei ^{74,76}Kr indicated well-deformed axially symmetric shapes at the lowest spins [1]; however, more recent works [2,3] show that shape coexistence plays an important role in the low-spin structure of these nuclei. Nuclei with two fewer protons, ^{72,74}Se, are nearly spherical at low spin but become deformed with increasing angular momentum, and are among the first nuclei in this region in which the phenomenon of shape coexistence was noted [4,5]. For many nuclei in the mass $A \approx 80$ region, cranked mean-field calculations predict triaxial deformations. Some of the nuclei for which this is the case are ^{74}Se [6], ^{76}Br [7,8], ^{77}Br [9], ^{78}Br [10], ^{79}Kr [11], and ^{82}Y [12].

Even though differences are often found in the structure of neighboring nuclei, the recent increase in the amount of systematic high-spin data has led to the realization that there are aspects of nuclear structure which are quite similar over a wide range of particle number, including moments of inertia at high spin [13] and the behavior of signature splitting and signature inversion in odd-odd nuclei [10].

The present work is an extension of a previous report by this group [14]. That work built upon previously published information about high-spin states in ^{76}Br [15–18] and extended the level scheme for both positive- and negative-parity rotational bands. The level scheme given in Ref. [14] was somewhat different than the one published earlier by Döring and co-workers [18]. Shortly after Ref. [14] was published, Buccino *et al.* [19] published a level scheme which was in agreement with that of Ref. [18]. In the present paper we will discuss in detail new data regarding the level scheme.

II. EXPERIMENTAL PROCEDURE

Two experiments were performed in which high-spin states in ^{76}Br were populated. In the first, the reaction ^{63}Cu (^{16}O,$n2p$) was used, using a 69 MeV ^{16}O beam from the Pittsburgh EN tandem. The second reaction used was ^{63}Cu (^{19}F,αpn), using a 67 MeV ^{19}F beam from the Notre Dame FN tandem. For both reactions, the target consisted of a pair of self-supporting ^{63}Cu foils, each 500 μg/cm^2 thick. In both experiments, the Pitt multidetector array [20] was used for γ-ray detection. This array consisted of six Compton-suppressed HPGe detectors and a 14-element BGO sum-multiplicity spectrometer (SMS). Events were defined by the firing of at least two HPGe detectors and at least two SMS elements. This latter requirement enhanced the selection of high-fold events. Events were collected on tape for later analysis. Approximately 30×10^6 coincidence events were collected in the ^{16}O reaction, and 44×10^6 coincidence events in the ^{19}F reaction. An additional 13×10^6 singles events, in which only one HPGe detector and no SMS elements were required, were collected in the ^{19}F reaction. The standard γ-ray sources ^{60}Co, ^{88}Y, ^{152}Eu, and ^{182}Ta were used for energy and efficiency calibration.

III. RESULTS

Total projections of the E_γ-E_γ matrices from the two reactions are shown in Fig. 1. Origins of the strong γ rays are indicated by symbols. As is typical in this mass region, there are several strong exit channels in the data. A partial level scheme for ^{76}Br, based on this and previous work, is shown in Fig. 2. The spin and parity of the ground-state band were established by Paradellis and co-workers [22] in a study of the decay of ^{76}Kr, and the 4^+ isomer upon which the yrast band is built was first established by Kreiner *et al.* [23]. Band 1 in Fig. 2 is the positive-parity yrast band, band 2 is the negative-parity band seen in previous work [18], and band 3 is the negative-parity band first reported in Ref. [14].

*Present address: Department of Radiology, University of Washington Medical Center, Seattle, Washington 98195.

†Present address: Instituto de Física da Universidade de São Paulo, São Paulo, Brasil.

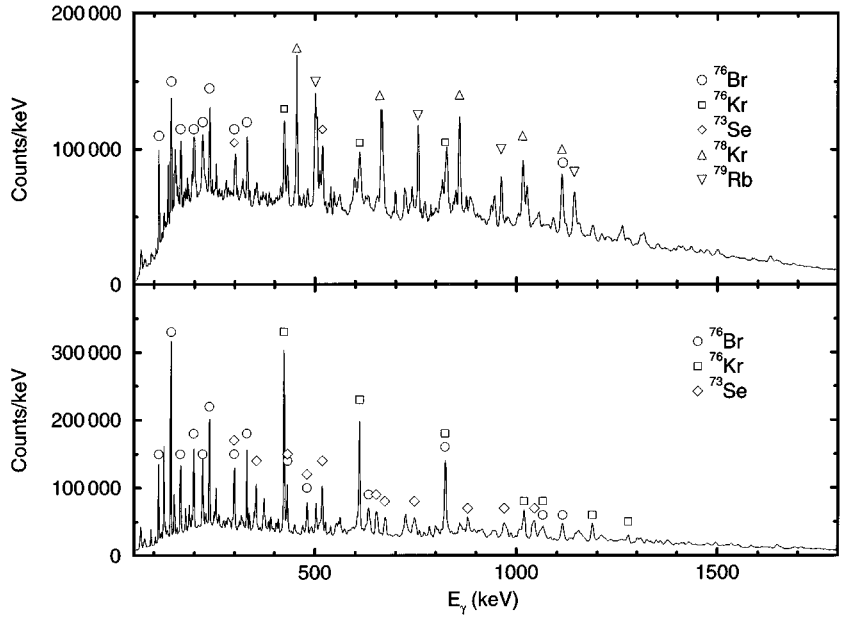

FIG. 1. Total projection of the E_γ-E_γ matrices from the ^{19}F (top) and ^{16}O (bottom) reactions. Symbols identify strong lines arising from the various reaction channels.

For clarity, the low-energy portion of the level scheme is reproduced with an expanded scale in Fig. 3. Intensities extracted from singles data are given in Table I. Because of the density of gamma-ray lines in the singles spectrum, only a few intensities could be reliably extracted.

The level scheme shown in Fig. 2 differs substantially from some previously published schemes [18,19] of high-spin phenomena in ^{76}Br, particularly in the positive-parity band. It is therefore necessary to discuss our assignments in some detail, paying particular attention to the points at which they differ from other published works.

A. Positive-parity band

The positive-parity band, which is yrast, decays to an isomeric 4^+ state at an energy of 102.7 keV. This band is believed to be built on a $\pi g_{9/2} \otimes \nu g_{9/2}$ structure [23]. A spectrum created by gating on several transitions in the positive-

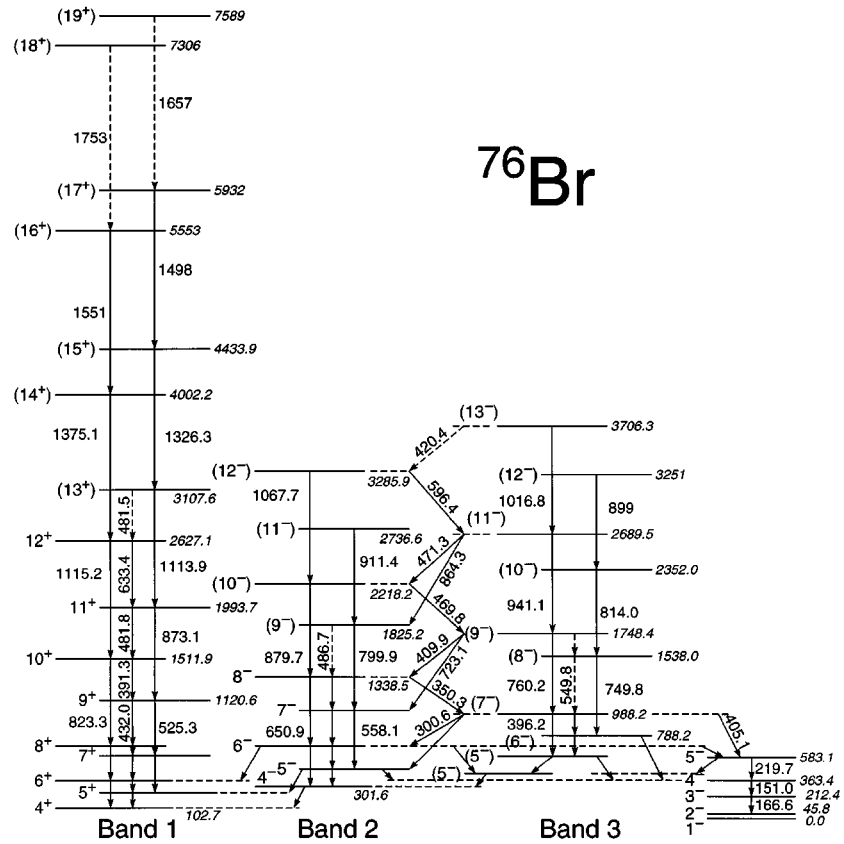

FIG. 2. Partial level scheme, based on this and previous work. The low-energy portion of the level scheme is reproduced with an expanded scale in Fig. 3.

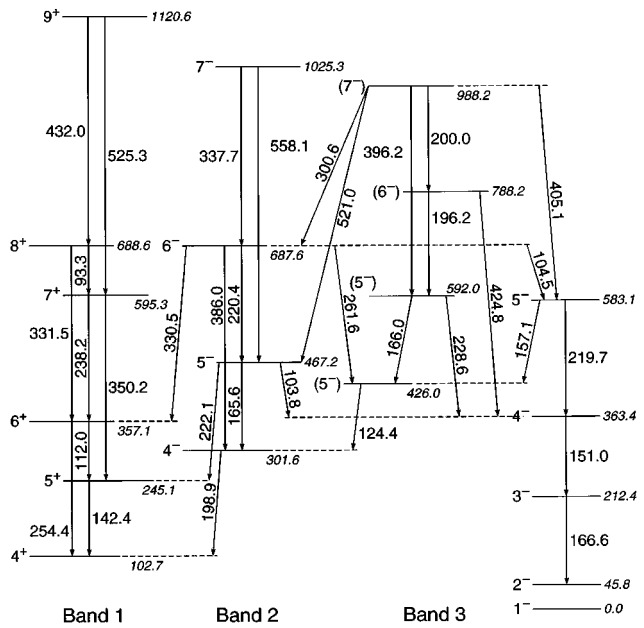

FIG. 3. Low-energy portion of the level scheme shown in Fig. 2.

parity band is shown in Fig. 4. A new transition has been added at the top of both positive-parity rotational sequences.

The most significant differences between our level scheme and those of Refs. [18,19] occur in the positive-parity yrast band. For comparison, we show the positive-parity band as given in Fig. 2 on the left-hand side of Fig. 5 along with the scheme of Buccino *et al.* [19] on the right-hand side of Fig. 5. Below spin 10, the schemes are identical. While Buccino *et al.* have a 1066 keV $12^+ \rightarrow 10^+$ transition, a 1258 keV $14^+ \rightarrow 12^+$ transition, and a 1374 keV $16^+ \rightarrow 14^+$ transition in the $\alpha = 0$ signature partner of the band, we see a 1115 keV $12^+ \rightarrow 10^+$ transition and a 1375 keV $14^+ \rightarrow 12^+$ transition. In our scheme, the $12^+ \rightarrow 10^+$ and $13^+ \rightarrow 11^+$ transitions comprise a doublet in the gamma spectrum at an energy of 1115 keV.

TABLE I. Intensities for gamma rays observed in this work, determined from singles data. No correction has been made for internal conversion.

E_γ (keV)	I_i^π	I_f^π	Intensity [a]
142	5^+	4^+	100 (5)
112	6^+	5^+	83 (8)
254	6^+	4^+	17 (2)
238	7^+	6^+	44 (3)
331	8^+	6^+	38 (4)
350	7^+	5^+	7 (1)
432	9^+	8^+	32 (3)
482	11^+	10^+	9 (1)
386	6^-	4^-	11 (2)
301	(7^-)	6^-	19 (1)

[a]Normalized to the 142 keV transition.

The reasons why we make our assignments as we do, and why we believe the assignments of Ref. [19] cannot be correct, are as follows: We do not see the 1066 keV or 1258 keV transitions in coincidence with either the 1375 or 391 keV transitions. This would be highly unlikely given the scheme shown on the right side in Fig. 5. In the top panel of Fig. 6, a spectrum created by gating on the 391 keV line is shown. Vertical arrows indicate the expected positions of 1066 keV and 1258 keV transitions. They are clearly not observed in this spectrum. We do see 1066 and 1258 keV transitions in weak coincidence with some of the lower-lying transitions, namely, the 142, 238, and 432 keV transitions. However, we do not see the 1066 and 1258 keV lines in coincidence with each other. From this, we conclude that these transitions feed independently into the yrast band at the 9^+ level, either directly or through intermediate transitions. A gate placed on the 1258 keV transition produces a spectrum showing transitions below the 9^+ state and no other lines of appreciable strength. A gate on the 1066 keV transition shows the lower portion of the yrast band, as well as several lines from one of the negative-parity bands and sev-

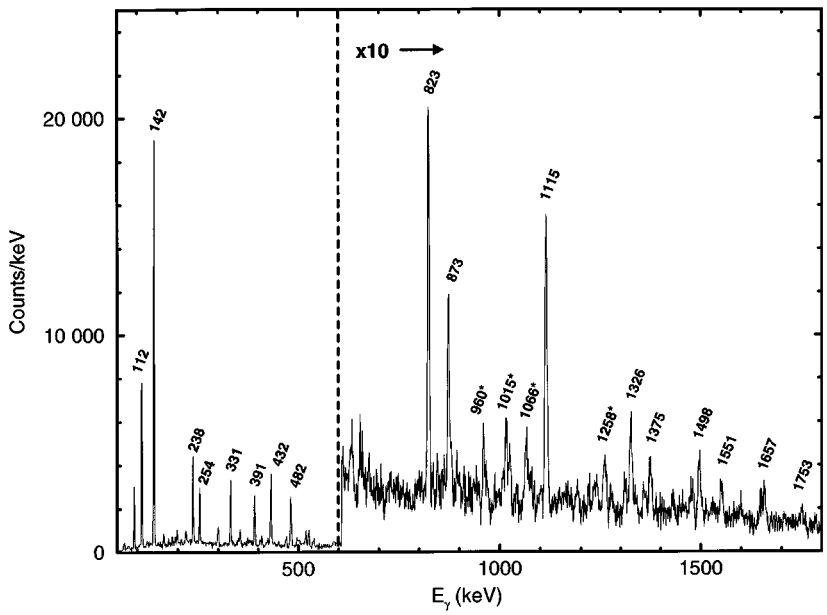

FIG. 4. Spectrum created by gating on transitions in the positive-parity band. Gates were placed on the 238, 350, and 432 keV lines. Asterisks indicate transitions that could not be placed in the level scheme.

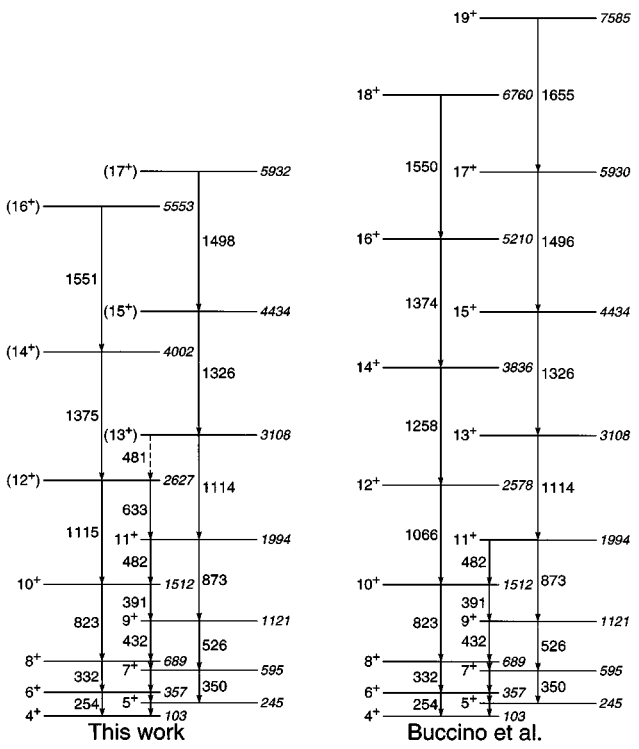

FIG. 5. Comparison of the yrast bands from this work and that of Buccino *et al.* [19].

eral lines from ^{76}Kr. These latter lines are present because the 1066 keV transition is close in energy to a 1068 keV transition in a negative-parity band of ^{76}Br and a 1067 keV transition in ^{76}Kr.

As for the 1115 keV line being a doublet, we offer the following arguments: We found the 1115 keV transition to be in strong coincidence with the 1375 keV transition. Given the level scheme shown on the right-hand side of Fig. 5, this would require a strong 728 keV $14^+ \rightarrow 13^+$ transition, which is not observed in any coincidence gate. In a spectrum created by gating on the 823 keV transition, it was found that the 1115 keV line was twice as strong as the 482 keV line, which is again inconsistent with the level scheme given in Ref. [19]. This can be seen in Fig. 6, where a spectrum created by gating on the 823 keV line is shown in the lower panel. Note that while the areas of the 482 keV and 1115 keV peaks in this spectrum are roughly equal, the efficiency of the detector array is only about half as much at the higher energy as compared to the lower. Finally, in spectra created by gating on the 1326 and 1375 keV transitions, the centroid of the 1115 keV peak is found to be different by 1.3 keV, as shown in Fig. 7. Based on these observations, we conclude that the strong line near 1115 keV is in fact a doublet and corresponds to the transitions as shown in the level scheme shown in Fig. 2.

In addition to the 1066 and 1258 keV transitions, we also see lines at 960 keV and 1015 keV in coincidence with the lower transitions in the positive-parity band, as indicated in the spectrum in Fig. 4. These transitions feed the band near the 9^+ level, but could not be placed with any confidence in the level scheme.

B. Negative-parity bands

Two negative-parity bands have been observed in ^{76}Br. The strongest of these feeds into a 4^- state at 302 keV of excitation, which has a half-life of 0.5 ns and decays to the 4^+ isomeric state via a 199 keV transition [18]. A spectrum created by gating on the 199 keV line is shown in Fig. 8. In Ref. [14] two transitions were added to this band to extend it to a spin of $12\hbar$. The two new transitions added were the 911 keV $(11^-) \rightarrow (9^-)$ transition and the 1068 keV $(12^-) \rightarrow (10^-)$ transition. A new rotational sequence, believed to be negative parity, was also reported in Ref. [14]. This sequence consisted of four new states with three in-band transitions of energy 760 keV, 941 keV, and 1017 keV, as well as several interband transitions to the previously known negative-parity band.

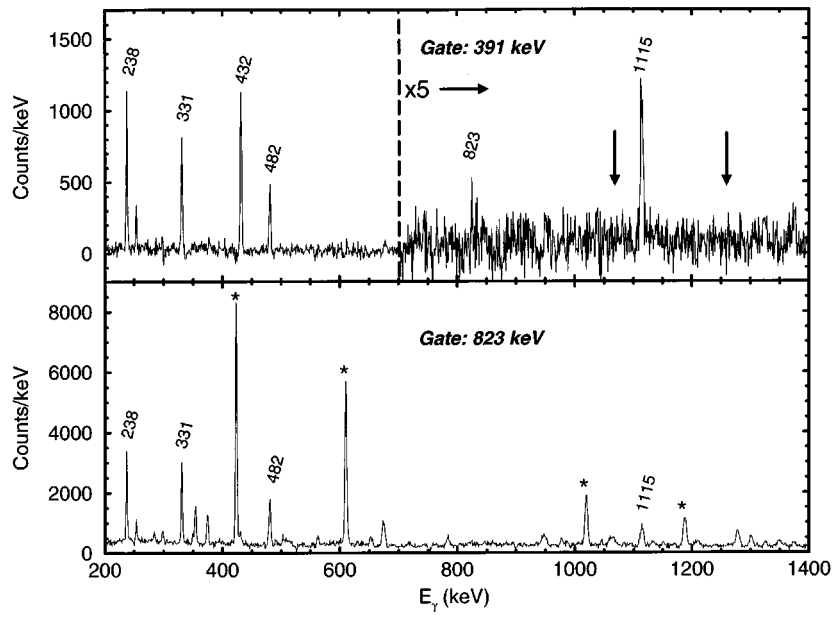

FIG. 6. The top panel shows a spectrum created by gating on the transition at 391 keV. Vertical arrows indicate the expected positions of 1066 and 1258 keV lines. The bottom panel shows a spectrum created by gating on the 823 keV transition. Asterisks indicate lines from the yrast band in ^{76}Kr, which contains an 824 keV transition.

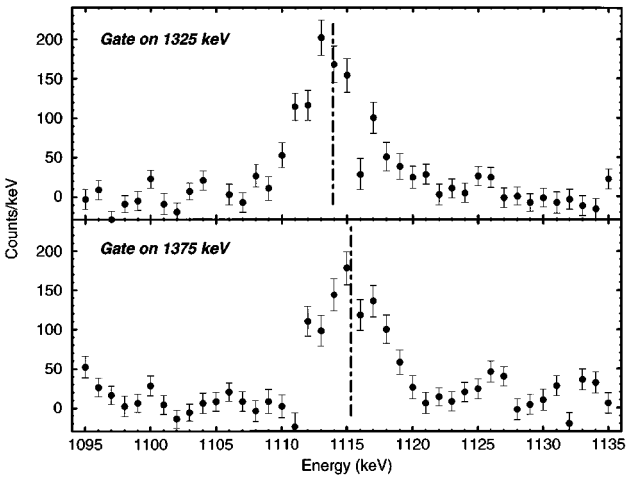

FIG. 7. Spectra created by gating on the 1325 keV (top) and 1375 keV (bottom) transitions. Centroids of the peak near 1115 keV are shown as dot-dashed lines. Uncertainties in the values of these centroids are 0.2 keV.

In the present work, several new transitions and levels in the negative-parity portion of the decay scheme are added. Placement of new levels was somewhat difficult due to the large number of doublets. Based on coincidence relationships, four of the new levels, at 788, 1538, 2352, and 3251 keV of excitation, appear to comprise the signature partner to the new rotational sequence found in Ref. [14]. These sequences are labeled ''band 3'' in Fig. 2.

Several high-energy transitions seen in Fig. 8 were too weak to place reliably in the level scheme. The 1145 and 1513 keV transitions are in coincidence with each other, as are the 1231 and 1472 keV transitions. All of these feed into the negative-parity bands at or above the (12^-) level at 3286 keV. The 1037 keV transition feeds the negative-parity band at or above the (10^-) level at 2218 keV. The 1314 keV transition feeds band 3 above the (13^-) level.

An additional new level at an excitation energy of 426 keV was also found. This level is fed by transitions from the 6^- level at 688 keV and the (5^-) level at 593 keV, and decays to the 4^- level at 382 keV; therefore, a tentative assignment of $I^\pi=(5^-)$ has been made for this level.

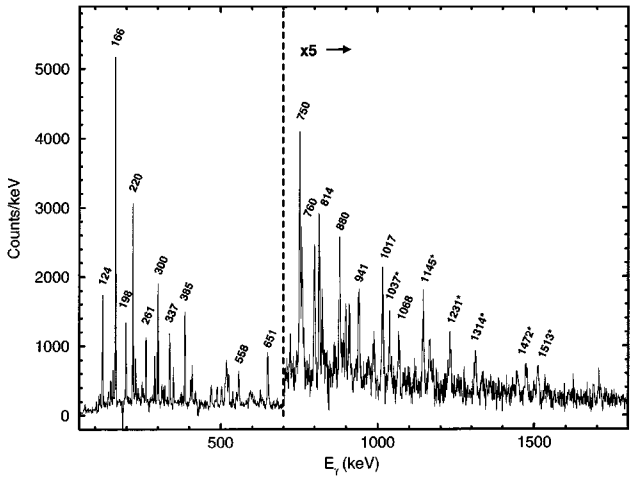

FIG. 8. Spectrum created by gating on the 199 keV line. Asterisks indicate transitions that could not be placed in the level scheme.

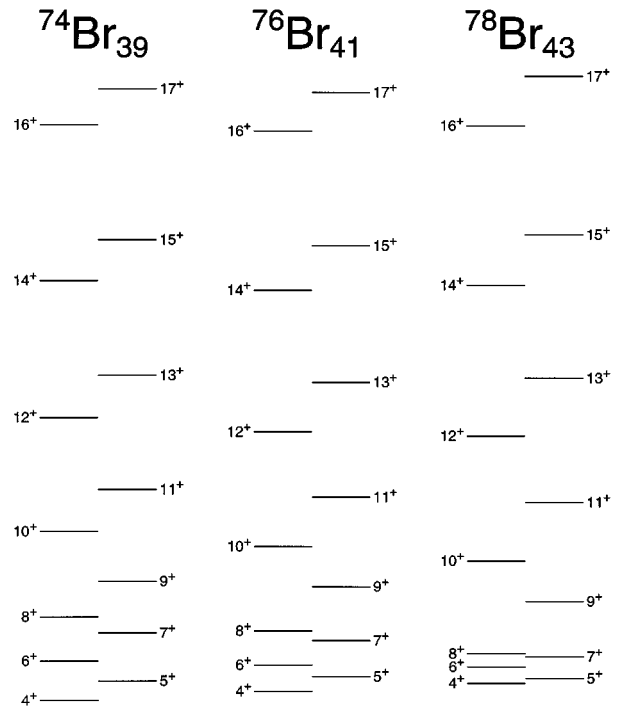

FIG. 9. Comparison of the level structure of the positive-parity bands in ^{74,76,78}Br.

IV. DISCUSSION

A. Systematics

While it is known that, quite often, nuclear structure properties in the $A\approx80$ vary rapidly with a change in nucleon number, there are instances in which similar structures persist over a wide range of neutron or proton numbers [10,13]. One example of this is shown in Fig. 9, in which the level

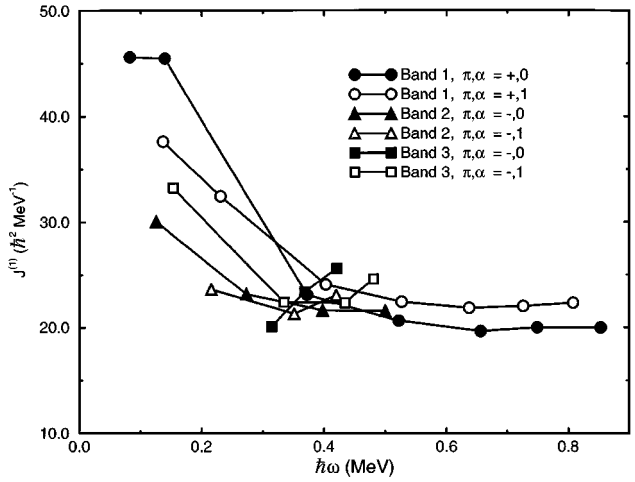

FIG. 10. Kinematic moments of inertia as a function of frequency.

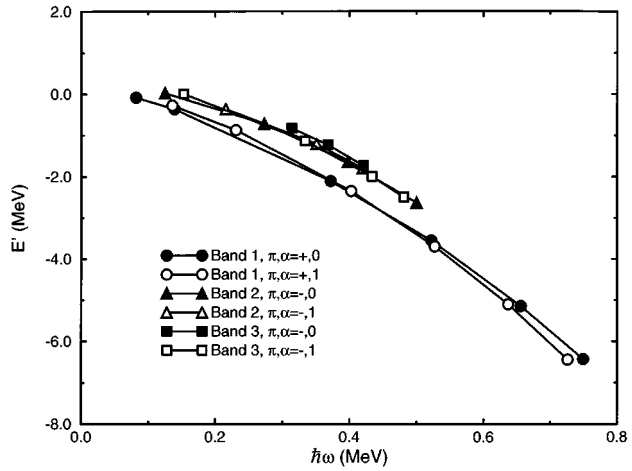

FIG. 11. Experimental Routhians as a function of frequency.

schemes of the positive-parity bands in ^{74}Br [21], ^{76}Br, and ^{78}Br [10] are compared with each other. Two features are immediately apparent in this comparison. First, as the neutron number approaches the $N=50$ closed shell, the spacing between states below about $I=10\hbar$ decreases. Second, at higher spin the level schemes of the three bands are nearly identical.

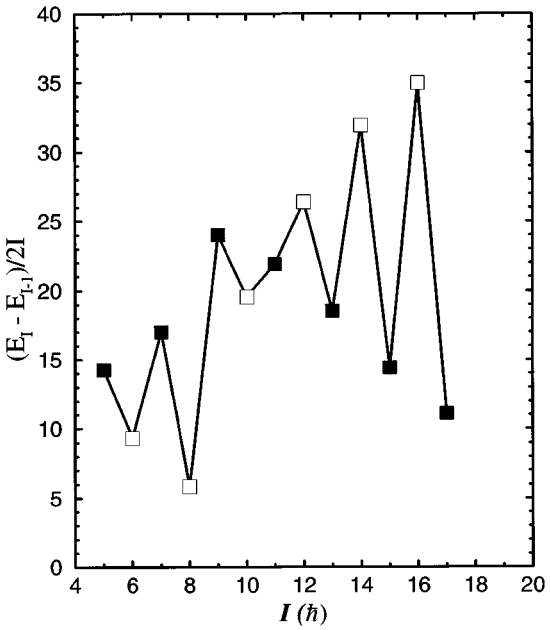

FIG. 12. Plot of the quantity $(E_I-E_{I-1})/2I$ as a function of spin for the yrast band in ^{76}Br.

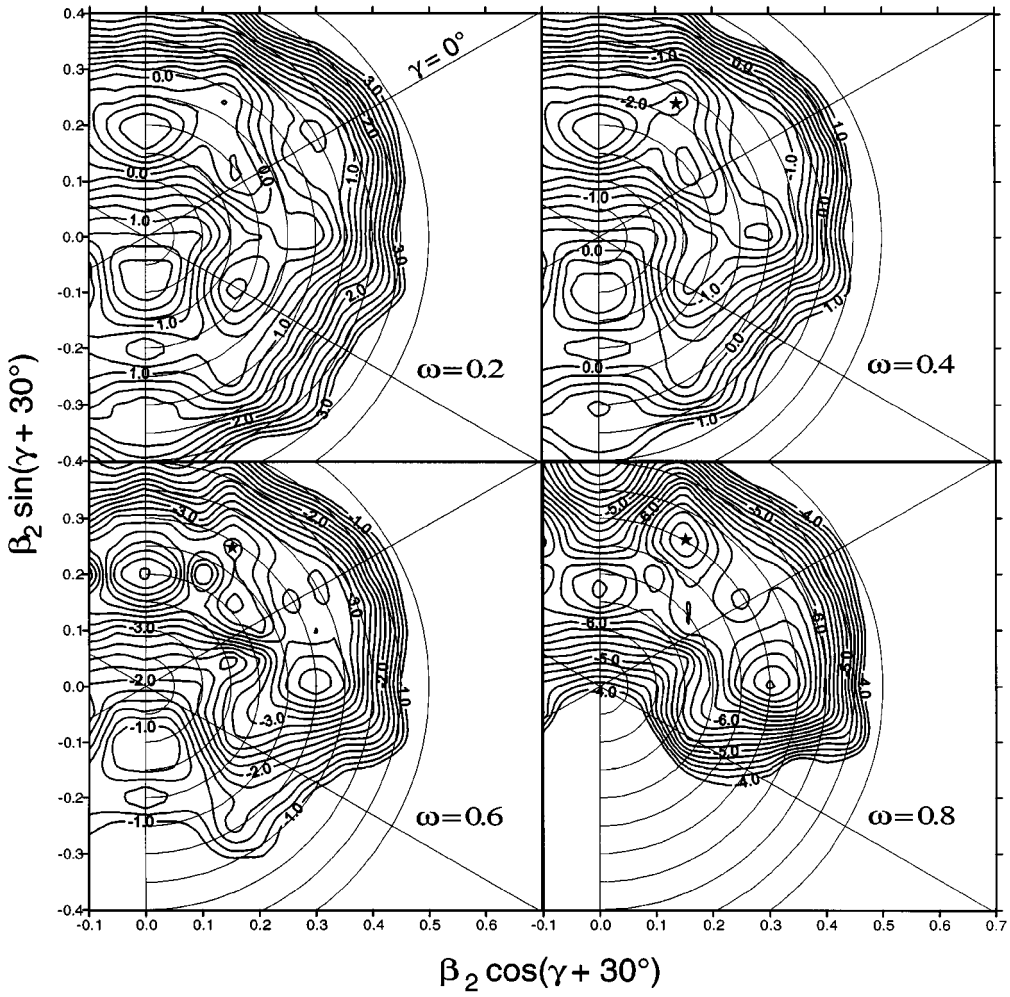

FIG. 13. Total Routhian surfaces for four rotational frequencies, calculated with self-consistent pairing at all frequencies. The deformation parameter β_4 was chosen to minimize the energy at each point. The frequency ω for each plot is indicated, in units of MeV/$\hbar$. A star indentifies the positive-gamma minimum used in the calculation of moment of inertia (Fig. 15) and signature splitting (Fig. 16).

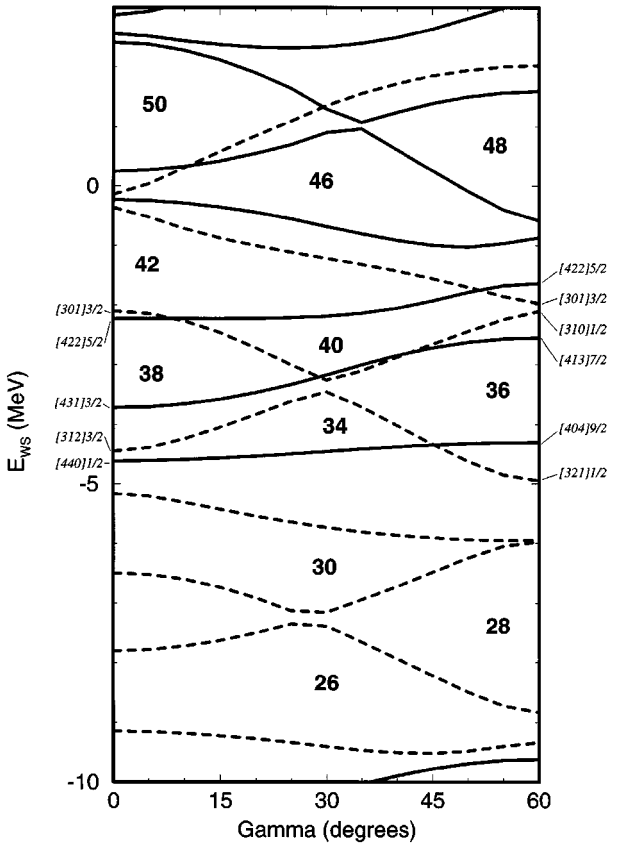

FIG. 14. Woods-Saxon levels as a function γ, for a fixed β_2 of 0.3. Nilsson quantum numbers associated with the orbitals at axially symmetric shape are indicated for the some of the levels.

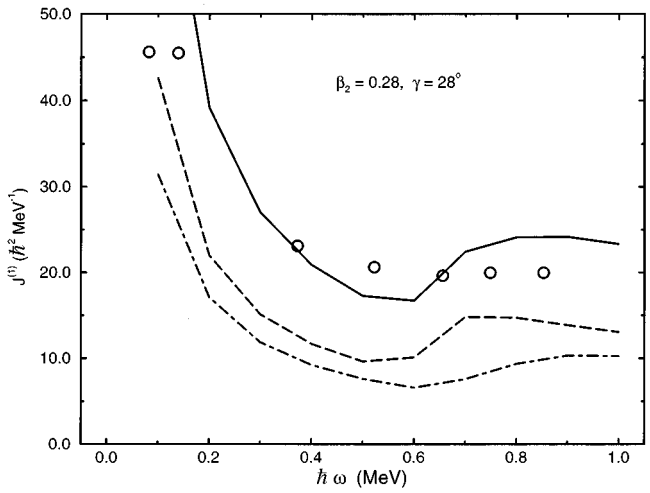

FIG. 15. Comparison of the calculated kinematic moment of inertia (solid line) to experimental values (circles), for the $(\pi,\alpha)=(+,0)$ sequence. The dashed line indicates the proton contribution to the calculated value, and the dot-dashed line the neutron contribution.

At low spin, the level spacing is dependent on the amount of mixing between states. For the lighter nuclei, the Fermi level lies nearer to the $\Omega=1/2$ suborbital low in the $g_{9/2}$ shell. This allows mixing of the Nilsson orbitals and results in level repulsion and more widely separated states. At higher spin, the position of the Fermi level becomes less important. For all of the nuclei, the protons occupy orbitals low in the $g_{9/2}$ shell, primarily the [431]3/2 and [440]1/2 orbitals. The Fermi level for neutrons is higher in the shell, near the [422]5/2 orbital. However, because of triaxiality and rotation, these orbitals and higher ones become well mixed for states of high angular momentum. Woods-Saxon calculations, which will be discussed in Sec. IV C, show that at deformations near $(\beta_2,\gamma) = (0.30,30°)$ the positive-parity level at the Fermi surface for neutrons is primarily [422]5/2, with large admixtures of [440]1/2 and [413]7/2 orbitals. It is likely that, at high angular momentum, the neutron states near the Fermi surface are well mixed, leading to the similarities in the level schemes.

B. Cranking model analysis

A cranking model analysis [24] was applied to the rotational bands. Figure 10 shows a plot of the kinematic moment of inertia, $\mathfrak{I}^{(1)}$, as a function of angular frequency for the rotational sequences seen in this work. As is typical for odd-odd nuclei in this region [13], the moments of inertia for most of the bands are high at low frequency, and converge to a value near the rigid-body value at higher frequency. The large value for $\mathfrak{I}^{(1)}$ at low spin in these nuclei arises from the single-particle motion of the unpaired nucleons; alignment of these particles with the rotational axis is energetically ''inexpensive'' and so appears as a large moment of inertia in the cranking interpretation. The $\alpha=0$ partner in band 3 shows an increasing moment of inertia throughout its frequency range, and the $\alpha=1$ sequences in bands 2 and 3 show upbends at their highest frequencies.

As mentioned previously, the yrast $K^{\pi}=4^{+}$ band is believed to be built on a $\pi g_{9/2}\otimes\nu g_{9/2}$ configuration. Thus, low-frequency crossings involving positive-parity orbitals are blocked. The negative-parity bands are most likely built on orbitals with one odd particle (proton or neutron) in a $g_{9/2}$ orbital, and the other in a negative-parity f or p orbital. Thus the upbends seen in bands 2 and 3 are likely due to an alignment in the unblocked $g_{9/2}$ orbital. Alignments near a frequency of $\hbar\omega=0.5$ MeV are seen in the yrast bands of both ^{75}Br [25] and ^{75}Se [26]. In both cases, the upbends are attributed to an alignment of $g_{9/2}$ orbitals for the unblocked nucleons (neutrons in ^{75}Br, protons in ^{75}Se). Because of this, an unambiguous assignment of the excited negative-parity bands in ^{76}Br is difficult. In any case, the strong interband transitions between these bands makes it likely that their configurations are similar. On the basis of the relative alignments of the positive- and negative-parity rotational sequences, Döring *et al.* [18] argue for a $\pi g_{9/2}\otimes\nu$ ($p_{3/2}$ or $f_{5/2}$) configuration for the negative-parity band observed in that work (band 2).

Experimental Routhians for the rotational sequences are shown in Fig. 11. No reference was subtracted in calculating these values; shape coexistence and polarization in this mass region make the choice of a meaningful reference problematical. The signature inversion in the positive-parity band can be seen in the crossing of the Routhians for the $\alpha=0$ and $\alpha=1$ signature partners (solid and open circles, respec-

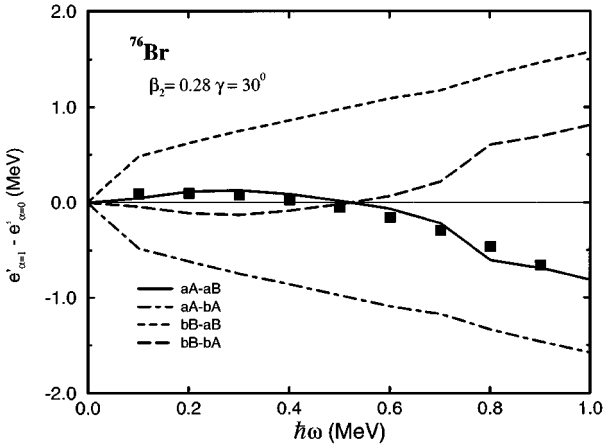

FIG. 16. Calculated and experimental signature splitting.

tively). The signature splitting and inversion can be seen more clearly by plotting the experimental quantity $(E_I - E_{I-1})/2I$ as a function of spin, as shown in Fig. 12. In this plot signature inversion can be seen as a reversal in the phase of the staggering at a spin of $9\hbar$. This inversion has been explained in the past [12,23,21] in terms of the gradual alignment of the unpaired nucleons to a maximum intrinsic spin of $9\hbar$. Above this spin the rotational band is generated by collective motion. These arguments are based on a particle-rotor approach. Recently, it has been shown that signature inversion can also be explained, in some cases, with cranked mean-field calculations [10], in agreement with earlier work by Bengtsson and co-workers [29]. Similar results will be discussed in the following section.

C. Calculations

In order to better understand the nature of the collective excitations observed in this experiment, theoretical model calculations were performed using a cranked Woods-Saxon potential, monopole pairing, and Strutinsky shell correction. For a more detailed discussion of the model, see Refs. [27,28] and references quoted therein. Calculated total Routhian surfaces (TRS's) for positive parity are shown in Fig. 13. The Lund convention was used for the shape parametrization, so that $\gamma = 0°$ is collective prolate, $\gamma = 60°$ is non-collective oblate, and $\gamma = -60°$ is collective oblate rotation. Self-consistency in the pairing was required at all frequencies, and β_4 was chosen to minimize the energy at each deformation point. There are clearly several shape-coexistent minima, including triaxial minima which persist throughout the range of frequencies shown. These minima appear at $\beta_2 \approx 0.3, \gamma \approx \pm 30°$. One reason for the stable triaxial shapes predicted in this region can be seen in Fig. 14, which shows Woods-Saxon levels as a function of γ for a constant value of $\beta_2 = 0.3$. Gaps between the levels at particle number 34 and 40 near $\gamma = 30°$ serve to stabilize triaxial shapes in nuclei with N or Z near these values. As mentioned before, ^{74}Se ($Z = 34, N = 40$) has been predicted to be triaxial [6].

Because self-consistent pairing is required at all frequencies, a direct comparison of experimental and calculated moments of inertia is possible, as shown in Fig. 15 for ^{76}Br. There is reasonable agreement between the theoretical values, shown as a solid line, and the experimental points. However, because states of different spin are mixed near crossing frequencies in this model, pairing often drops off more rapidly than is realistic. This is manifested in this case by the sharp upbend at high frequency in the calculated moment of inertia. The calculations were done using the deformation parameters from the TRS minimum at $\beta_2 = 0.28, \gamma = 28°$, corresponding to the positive-gamma triaxial minimum of Fig. 13. While calculations using the the negative-γ triaxial minimum also give reasonable agreement for the moment of inertia, the positive-γ parameters were used here because they give a better characterization of the signature splitting, as described below. It should be noted that the only adjustable parameters used in the calculation, the pairing strengths G for protons and neutrons, are adjusted to give the best fit to the moment of inertia. The values used in this work are $22.8/A$ MeV for protons and $21.4/A$ MeV for neutrons.

In the past, the signature inversion has most often been discussed in the framework of particle-rotor models. However, Bengtsson *et al.* [29] suggested that, for certain particle numbers, a signature-inverted spectrum can be obtained in the cranked mean-field approach when a triaxially deformed nucleus is cranked around the shortest axis ($\gamma > 0°$ in the Lund convention). The calculated and experimental signature splitting is shown in Fig. 16 for the yrast band of ^{76}Br. Once again, a deformation of $\beta_2 = 0.28$, $\gamma = 28°$ was used in the calculation. The differences between the Routhians for the $\alpha = 1$ signature partner and the $\alpha = 0$ signature partner are plotted as a function of angular frequency. Symbols indicate the experimentally derived values, and the four lines in each panel show the calculated quantities based on the four possible combinations of configuration. Lowercase letters indicate the proton configuration, uppercase the neutron configuration. The letters a (or A) and b (or B) refer to the lowest positive-parity Routhians with signature $\alpha = 1/2$ or $\alpha = -1/2$, respectively. There is good agreement between the experimental points and the calculated values for the aA-aB configuration pair, in both the magnitude of the splitting and the frequency at which the inversion occurs. A similar analysis has been applied to neighboring nuclei in Ref. [10].

V. SUMMARY AND CONCLUSIONS

Several new transitions and excited states were found in ^{76}Br, using two different fusion-evaporation reactions. Cranked mean-field calculations with self-consistent pairing suggest a triaxial shape for the positive-parity band. Signature inversion is well reproduced by the calculations.

ACKNOWLEDGMENTS

This work was funded by the National Science Foundation. The cranked shell model codes used in this work were provided by Prof. J. Dudek of Strasbourg.

[1] R. B. Piercey, J. H. Hamilton, R. Soundranayagam, A. V. Ramayya, C. F. Maguire, X.-J. Sun, Z. Z. Zhao, R. L. Robinson, H. J. Kim, S. Frauendorf, J. Döring, L. Funke, G. Winter, J. Roth, L. Cleeman, J. Eberth, W. Neumann, J. C. Wells, J. Lin, A. C. Rester, and H. K. Carter, Phys. Rev. Lett. **47**, 1514 (1981).

[2] S. L. Tabor, P. D. Cottle, J. W. Holcomb, T. D. Johnson, P. C. Womble, S. G. Buccino, and F. E. Durham, Phys. Rev. C **41**, 2658 (1990).

[3] J. Heese, D. J. Blumenthal, A. A. Chishti, P. Chowdhury, B. Crowell, P. J. Ennis, C. J. Lister, and Ch. Winter, Phys. Rev. C **43**, R921 (1991).

[4] J. H. Hamilton, A. V. Ramayya, W. T. Pinkston, R. M. Ronningen, G. Garcia-Bermudez, H. K. Carter, R. L. Robinson, H. J. Kim, and R. O. Sayer, Phys. Rev. Lett. **32**, 239 (1974).

[5] R. M. Ronningen, A. V. Ramayya, J. H. Hamilton, W. Lourens, J. Lange, H. K. Carter, and R. O. Sayer, Nucl. Phys. **A261**, 439 (1976).

[6] P. D. Cottle, J. W. Holcomb, T. D. Johnson, K. A. Stuckey, S. L. Tabor, P. C. Womble, S. G. Buccino, and F. E. Durham, Phys. Rev. C **42**, 1254 (1990).

[7] D. F. Winchell, Ph.D. thesis, University of Pittsburgh, 1990 (unpublished).

[8] L. Wehner, Ph.D. thesis, University of Pittsburgh, 1994 (unpublished).

[9] G. N. Sylvan, J. E. Purcell, J. Döring, J. W. Holcomb, G. D. Johns, T. D. Johnson, M. A. Riley, P. C. Womble, V. A. Wood, and S. L. Tabor, Phys. Rev. C **48**, 2252 (1993).

[10] E. Landulfo, D. F. Winchell, J. X. Saladin, F. Cristancho, D. E. Archer, J. Döring, G. D. Johns, M. A. Riley, S. L. Tabor, V. A. Wood, S. Salém-Vasconcelos, and O. Dietzsch, Phys. Rev. C **54**, 626 (1996).

[11] R. Schwengner, J. Döring, L. Funke, G. Winter, A. Johnson, and W. Nazarewicz, Nucl. Phys. **A509**, 550 (1990).

[12] P. C. Womble, J. Döring, T. Glasmacher, J. W. Holcomb, G. D. Johns, T. D. Johnson, T. J. Petters, M. A. Riley, V. A. Wood, S. L. Tabor, and P. Semmes, Phys. Rev. C **47**, 2546 (1993).

[13] S. L. Tabor, Phys. Rev. C **45**, 242 (1992).

[14] D. F. Winchell, J. X. Saladin, M. S. Kaplan, and H. Takai, Phys. Rev. C **41**, 1264 (1990).

[15] M. Behar, A. Filevich, G. Garcia-Bermudez, and M. A. J. Mariscotti, Nucl. Phys. **A282**, 331 (1977).

[16] W. D. Schmidt-Ott, A. J. Hautojarvi, and U. J. Schrewe, Z. Phys. A **289**, 121 (1978).

[17] J. C. Wells, R. L. Robinson, H. J. Kim, R. O. Sayer, R. B. Piercey, A. V. Ramayya, J. H. Hamilton, C. F. Maguire, K. Kumar, R. W. Eastes, M. E. Barclay, and A. J. Caffrey, Phys. Rev. C **24**, 171 (1981).

[18] J. Döring, G. Winter, L. Funke, P. Kemnitz, and E. Will, Z. Phys. A **305**, 365 (1982).

[19] S. G. Buccino, F. E. Durham, J. W. Holcomb, T. D. Johnson, P. D. Cottle, and S. L. Tabor, Phys. Rev. C **41**, 2056 (1990).

[20] J. X. Saladin, IEEE Trans. Nucl. Sci. **NS-30**, 420 (1983).

[21] J. W. Holcomb, T. D. Johnson, P. C. Womble, P. D. Cottle, S. L. Tabor, F. E. Durham, and S. G. Buccino, Phys. Rev. C **43**, 470 (1991).

[22] T. Paradellis, A. Houdayer, and S. K. Mark, Nucl. Phys. A **A201**, 113 (1973).

[23] A. J. Kreiner, G. Garcia-Bermudez, M. A. J. Mariscotti, and P. Thieberger, Phys. Lett. **83B**, 31 (1979).

[24] R. Bengtsson, S. Frauendorf, and F.-R. May, At. Data Nucl. Data Tables **35**, 15 (1986).

[25] N. Martin, C. J. Gross, J. Heese, and K. P. Lieb, J. Phys. G **15**, L123 (1989).

[26] T. D. Johnson, T. Glasmacher, J. W. Holcomb, P. C. Womble, S. L. Tabor, and W. Nazarewicz, Phys. Rev. C **46**, 516 (1992)

[27] W. Nazarewicz, J. Dudek, R. Bengtsson, T. Bengtsson, and I. Ragnarsson, Nucl. Phys. **A435**, 397 (1985).

[28] D. F. Winchell, M. S. Kaplan, J. X. Saladin, H. Takai, J. J. Kolata, and J. Dudek, Phys. Rev. C **40**, 2672 (1989).

[29] R. Bengtsson, H. Frisk, F. R. May, and J. A. Pinston, Nucl. Phys. **A415**, 189 (1984).